horticulturae

MDPI

Article

Non-Enzymatic and Enzymatic Antioxidant Responses of *Hypericum perforatum* L. Hairy Roots upon Photooxidative Stress

Oliver Tusevski and Sonja Gadzovska Simic *

Institute of Biology, Faculty of Natural Sciences and Mathematics, University "Ss. Cyril and Methodius" in Skopje, 1000 Skopje, North Macedonia
* Correspondence: sonjag@pmf.ukim.mk

Abstract: The aim of this study was to evaluate the non-enzymatic and enzymatic antioxidant response of fifteen *Hypericum perforatum* L. dark-grown (HR1 A-HR1 O) and photoperiod-exposed (HR2 A-HR2 O) hairy root clones. Dark-grown HR1 clones were characterized with high biomass accumulation and up-regulated phenylpropanoid metabolism through phenylalanine ammonia lyase (PAL)-mediated production of flavonoids, flavan-3-ols and anthocyanins. These groups of phenolics showed superior hydrogen-donating capability and significantly contributed to the antioxidant capacity of dark-grown HR1 clones. Photoperiod-exposed HR2 clones showed green coloration with shoot regenerative potential and reduced biomass accumulation. Photoperiod exposition improved the production of hypericins, as well as ferrous chelating properties and lipid peroxidation inhibition activity in HR2 cultures. Furthermore, HR2 clones were represented with enhanced activity of antioxidant enzymes (guaiacol peroxidase, catalase and superoxide dismutase) that resulted in suppression of oxidative stress markers (hydrogen peroxide, superoxide anion and malondialdehyde). These observations revealed the involvement of an efficient antioxidant defense system in the adaptive response of HR to photooxidative stress. Altogether, photoperiod-exposed *H. perforatum* HR2 clones were considered as a promising alternative for further scale-up production of naphthodianthrones that could be used in the pharmaceutical industry.

Keywords: antioxidant activity; hairy roots; *Hypericum perforatum* L.; phenolics; photoperiod

Citation: Tusevski, O.; Gadzovska Simic, S. Non-Enzymatic and Enzymatic Antioxidant Responses of *Hypericum perforatum* L. Hairy Roots upon Photooxidative Stress. *Horticulturae* **2023**, *9*, 581. https://doi.org/10.3390/horticulturae9050581

Academic Editor: Lucia Guidi

Received: 21 February 2023
Revised: 15 March 2023
Accepted: 21 March 2023
Published: 13 May 2023

1. Introduction

Hypericum perforatum L. (St. John's wort) is recognized as the most important medicinal plant all over the world. The *H. perforatum* extracts represent a rich source of naphthodianthrones, acyl-phloroglucinols, flavonoids, hydroxycinnamic acids and xanthones that are responsible for antidepressant, antioxidant, antimicrobial, antiviral, anti-inflammatory and anticancer activities [1]. The pharmaceutical industry is presently supplied with the upper flowering parts of wild-growing or cultivated plants for preparation of *H. perforatum* commercial remedies [2]. However, the obtainment of crude extracts with a stable quantity of bioactive compounds is still difficult due to the influence of various abiotic and biotic environmental factors on the phytochemical composition of field-grown plants [3]. In addition, the heterogeneity of secondary metabolite contents is greatly influenced by the genotype, and developmental and physiological states, as well the harvesting period and processing of plant material [4]. Therefore, the application of biotechnological tools for cultivation of *H. perforatum* under controlled and aseptic conditions is a key prerequisite to obtain sustainable and high-quality biomass with standardized production of bioactive metabolites.

There is a plethora of studies reporting that *Hypericum* cell, tissue and organ cultures represent an efficient system for continuous production of pharmacologically active compounds. Phytochemical analyses of *H. perforatum* in vitro cultures have mainly been focused on shoots and plantlets as the richest sources of hypericins, hyperforins, phenolic

acids and various groups of flavonoids [5–8]. The capability of undifferentiated callus and cell suspension cultures for production of these shoot-specific phenolic compounds has also been studied [5,6,9]. On the other hand, *H. perforatum* root cultures that have previously been considered as an unattractive model for commercial exploitation have now become a promising experimental system for accumulation of valuable metabolites [10–13]. The production of various primary and secondary metabolites has previously been reported in *H. perforatum* root cultures elicited with chitosan [12]. Similarly, Tocci et al. [11] have observed that biomass production and xanthone accumulation in chitosan-elicited *H. perforatum* root cultures are dependent on auxin concentration in the medium. In addition, several studies have pointed out that optimization of bioreactor technology is a key point for increased growth and secondary metabolite accumulation in *H. perforatum* adventitious root cultures [10,14,15]. Although significant product yield of *H. perforatum* roots has been achieved through culture optimization, the obtainment of secondary-metabolite-enriched biomass needs further improvement for commercial scale-up production.

Agrobacterium-rhizogenes-mediated plant transformation represents a biotechnological approach that combines in vitro culture and "natural genetic engineering" technologies for the establishment of hairy roots (HR). The HR cultures have been proposed as a suitable system for large-scale biomass production due to their auxin-independent growth associated with strong biosynthetic capacity [16]. Despite the recalcitrant nature of the genus *Hypericum* to *Agrobacterium* transformation, there are several reports of successful establishment of HR cultures [17–20]. *Hypericum* HR cultures have been the subject of extensive studies concerning their phenotype and regenerative potential, as well as secondary metabolite production [19–26]. From our recent studies, *H. perforatum* HR cultures have been shown to represent an efficient source of phenolic acids, catechins, quercetin and kaempferol glycosides, as well as numerous xanthones with antioxidant, antimicrobial, antidepressant, neuroprotective and antidiabetic properties [19,24,26]. However, *Hypericum* HR were not always able to produce hypericins and hyperforins, which are usually accumulated in plant aerial parts [19,20,26]. It has been shown that HR cultures exposed to light or photoperiod turn green due to development of chloroplasts that might contribute to the capability for de novo production of shoot-specific compounds [27]. Results from our previous study showed that *H. perforatum* HR are responsive to photoperiodic stimulus through de novo biosynthesis and accumulation of hydroxycinnamic acids, flavonols and xanthones [28]. The data indicate that the biosynthetic potential of photoperiod-exposed HR has been activated due to stress-induced responses upon light exposure. The greening of HR could be considered as an unusual physiological phenomenon related to light-dependent production of reactive oxygen species (ROS). This oxidative burst triggers the non-enzymatic and enzymatic antioxidant machinery to combat the photooxidative stress in green HR [29]. Altogether, these observations lay down the current hypothesis that exposure of *H. perforatum* HR to light induces a complex array of plant defense responses through modulation of phenylpropanoid/naphthodianthrone metabolism and substantial modification of antioxidant status.

This is the first study to evaluate the antioxidant status of fifteen *H. perforatum* HR clones upon photooxidative stress. For this purpose, fifteen HR lines grown under dark and photoperiod conditions were analyzed according to the following topics:

(1) fresh weight, dry weight, fresh weight/dry weight ratio and dry weight yield;
(2) total phenolic, flavonoid, flavan-3-ol, anthocyanin and hypericin contents;
(3) phenylalanine ammonia lyase and polyphenol oxidase activities;
(4) cupric ion reducing antioxidant capacity, DPPH radical scavenging activity, ferrous chelating activity and lipid peroxidation inhibition;
(5) guaiacol peroxidase, catalase and superoxide dismutase activities;
(6) hydrogen peroxide, superoxide radical and malondialdehyde contents.

2. Materials and Methods

2.1. Establishment of Dark-Grown and Photoperiod-Exposed HR Clones

Solid-grown HR clones have been previously established by *A. rhizogenes* A4-mediated transformation of *H. perforatum* [19,25]. Fifteen HR clones derived from independent transformation events were denoted with capital letters (HR A-HR O). These HR lines were used here for establishment of dark-grown (HR1 A-HR1 O) and photoperiod-exposed (HR2 A-HR2 O) clones. For this purpose, 0.5 g of each solid-grown HR clone was inoculated into 100 mL liquid MS/B_5 medium in Erlenmeyer flasks (250 mL) and placed on a rotary shaker (100 rpm). The HR1 cultures were maintained in a culture room under darkness, while HR2 lines were exposed to photoperiod at 16 h light/8 h dark and irradiance of 50 µmol m^2 s^{-1}. A control experiment was set up with non-transformed roots cultured in liquid medium under darkness (NTR1) and photoperiod (NTR2).

2.2. Growth Characteristics

The HR1 and HR2 clones along with the corresponding control NTR1 and NTR2 roots were evaluated for fresh weight (FW), dry weight (DW), FW/DW ratio and dry weight yield (DWY). The HR (0.5 g) were cultured into liquid MS/B_5 medium for one month and the FW was measured. For determination of DW, the HR were lyophilized under vacuum (0.22 mbar). The values for FW and DW of HR cultures were used for determination of FW/DW ratio and DWY (DWY = DW/FW × 100).

2.3. Phenolic Compound Contents

One-month-old HR1 and HR2 clones of *H. perforatum* were harvested, frozen in liquid nitrogen, then lyophilized and stored at −80 °C, until phytochemical analyses. Phenolic compounds extraction and quantification were performed as previously reported [25]. The phenolic compound contents in plant extracts included determination of total phenolics (TP), flavonoids (TF), flavan-3-ols (TFA), anthocyanins (TA) and hypericins (TH). Spectrophotometric analyses were performed on a SpectraMax 190 Microplate Reader (Molecular Devices Corp., Sunnyvale, CA, USA) supported with SoftMax Pro (v. 5.4.1) software.

The TP contents in HR were determined by mixing root extracts with Folin–Ciocalteu reagent and 0.7 M sodium carbonate [30]. The samples were incubated at 50 °C for 15 min and then cooled at room temperature. The sample absorbance was measured at 765 nm and TP contents were expressed as milligrams of gallic acid (GA) equivalents per gram of dry weight (mg GA·g^{-1} DW).

The TF contents in HR were determined using the assay described by Zhishen et al. [31]. Root extract was mixed with 5% sodium nitrite, 10% aluminium chloride and 1 M sodium hydroxide. The sample absorbance was measured at 510 nm and TF contents were expressed as milligrams of catechin (C) equivalents per gram of dry weight (mg C·g^{-1} DW).

The TFA contents in HR were estimated by 4-dimethylaminocinnamaldehyde (DMACA) assay [32]. The 0.1% DMACA reagent was added to diluted root extracts. The sample absorbance was measured at 640 nm and TFA contents were expressed as milligrams of catechin (C) equivalents per gram of dry weight (mg C·g^{-1} DW).

The TA contents in HR were determined by the pH-differential method [33]. The root extracts were diluted with 0.025 M KCl (pH 1.0) and 0.4 M CH_3COONa (pH 4.5) buffers and incubated at room temperature for 20 min. The sample absorbance was measured at 510 nm and 700 nm. The molar extinction coefficient of cyanidin-3-glucoside (ε_{535} = 26,900 L·mol^{-1}·cm^{-1}) was used for determination of TA contents expressed as milligrams of cyanidin-3-glucoside (CG) equivalents per gram of dry weight (mg CG·g^{-1} DW).

The TH contents in HR were assayed using the protocol described in the study of Tusevski et al. [25]. The hypericins were extracted from a powdered sample using 80% tetrahydrofuran at 65 °C. After centrifugation, the supernatant was lyophilized under vacuum and the dried extracts were dissolved in CH_3OH. The methanolic extracts were centrifuged (10 min at 12,000 rpm) and the absorbance of the supernatant was read at

590 nm. The TH contents were expressed as micrograms of hypericin (H) equivalents per gram of dry weight (μg H·g^{-1} DW).

2.4. Phenylalanine Ammonia Lyase (PAL) and Polyphenol Oxydase (PPO) Activities

The extract for determination of phenylalanine ammonia lyase (PAL) and polyphenol oxidase (PPO) activities was prepared by homogenization of 0.3–0.4 g frozen root tissue in 1 mL suitable buffer. The homogenate was centrifuged at 13,000 rpm for 20 min at 4 °C and the supernatant was collected for determination of soluble protein content, as well as for PAL and PPO assays. The analysis of protein content in the enzyme extracts was performed with Bradford reagent. The reaction mixture consisting of the enzyme extract and Bradford reagent was incubated at room temperature for 10 min and the absorbance was measured at 595 nm. The total protein content in the enzyme extracts was calculated using bovine serum albumin as a standard.

The PAL assay in enzyme extracts was performed according to Gadzovska et al. [6] with modifications reported by Tusevski et al. [25]. The extraction of PAL enzyme from fresh HR tissue was done with 100 mM sodium borate buffer (pH 8.8). The mixture consisting of extraction buffer, enzyme extract and 20 mM L-phenylalanine was incubated at 40 °C. The increase of absorbance was monitored every 20 min for a period of 60 min at 290 nm. The molar extinction coefficient of trans-cinnamic acid (ε_{290} = 9630 L·mol^{-1}·cm^{-1}) was used for calculation of PAL activity in pkat·mg^{-1} proteins.

The PPO assay in enzyme extracts was performed according to the method of Das et al. [34] with modifications described by Tusevski et al. [25]. The extraction of PPO enzyme from fresh HR tissue was done with 50 mM potassium phosphate buffer (pH 7). The reaction mixture consisting of extraction buffer, enzyme extract and 40 mM pyrocatechol was incubated at room temperature. The increase of absorbance was monitored every 10 min for a period of 30 min at 390 nm. The molar extinction coefficient of 1,2-benzoquinone (ε_{390} = 1417 L·mol^{-1}·cm^{-1}) was used for calculation of PPO activity in nkat·mg^{-1} proteins.

2.5. Non-Enzymatic Antioxidant Capacity Assays

The antioxidant capacity of HR extracts was measured using the following methods: cupric ion reducing antioxidant capacity (CUPRAC), DPPH radical scavenging activity, ferrous chelating activity (FCA) and lipid peroxidation inhibition (LPI).

The CUPRAC assay was determined by the method of Apak et al. [35] that included mixing of HR extract, 10 mM $CuCl_2$, 7.5 mM neocuproine and 1 M ammonium acetate buffer (pH 7). After incubation for 30 min at room temperature, the absorbance of the samples was read at 450 nm. The molar extinction coefficient of trolox (ε_{535} = 1.67 × 10^4 L·mol^{-1}·cm^{-1}) was used for calculation of CUPRAC values expressed as micromoles of trolox (T) equivalents per gram of dry weight (μmol T·g^{-1} DW).

The DPPH assay was performed by evaluation of HR extracts to scavenge 0.25 mM 2,2-diphenyl-1-picrylhydrazyl radical (DPPH$^{\bullet}$) according to the method of Brand-Williams et al. [36]. In a control sample, the extract was replaced with CH_3OH. After incubation at room temperature in the dark for 10 min, the decrease in absorbance of the samples was recorded at 518 nm. The DPPH radical scavenging activity was expressed as micromoles of trolox (T) equivalents per gram of dry weight (μM T·g^{-1} DW).

The FCA was estimated by the method of Decker and Welch [37] that included mixing HR extracts with 2 mM $FeCl_2$ and 5 mM ferrozine. The sample absorbance was measured at 562 nm, and FCA was expressed as milligrams of ethylenediaminetetraacetic acid (EDTA) equivalents per gram of dry weight (mg EDTA·g^{-1} DW).

The LPI was determined according to the β-carotene bleaching method described by Sun and Ho [38]. A linoleic acid-β-carotene emulsion was prepared by mixing 20 mg linoleic acid with 0.2 mg·mL^{-1} β-carotene chloroformic solution and 200 mg Tween 40. Chloroform was evaporated under nitrogen flow for 10 min and the mixture was adjusted to a certain volume with distilled water. The mixture consisting of HR extracts and linoleic acid-β-carotene emulsion was incubated at 50 °C. In a control sample, the HR extract was

replaced with CH_3OH. The absorbance was monitored in 15 min for a period of 45 min at 470 nm. The LPI was expressed as inhibition of β-carotene bleaching according to the following formula: LPI [%] = ((B − A)/B) × 100, where A is variation in absorbance of samples between 0 and 45 min and B is variation in absorbance of control between 0 and 45 min.

2.6. Antioxidant Enzyme Activities

The activities of antioxidant enzymes guaiacol peroxidase (PX), catalase (CAT) and superoxide dismutase (SOD) were determined in enzyme extracts that were prepared by homogenization of frozen HR tissue with 50 mM potassium phosphate buffer (pH 7). Tissue homogenate was centrifuged at 13,000 rpm for 20 min at 4 °C and the supernatant was used for quantification of soluble proteins and antioxidant enzyme assays.

The PX activity was performed by mixing enzyme extract, 2% guaiacol and 0.3% hydrogen peroxide [39]. The increase of absorbance was observed every minute for a period of 5 min at 470 nm. The molar extinction coefficient of tetraguaiacol (ε_{470} = 26.6 $L \cdot mol^{-1} \cdot cm^{-1}$) was used for calculation of PX activity in $nkat \cdot mg^{-1}$ proteins.

The method for determination of CAT activity [40] was performed by addition of 0.1% hydrogen peroxide to diluted enzyme extract with 50 mM potassium phosphate buffer (pH 7). The absorbance decrease in the samples was monitored every 20 s for a period of 1 min at 240 nm. The molar extinction coefficient of hydrogen peroxide (ε_{240} = 43.6 $L \cdot mol^{-1} \cdot cm^{-1}$) was used to express CAT activity in $nkat \cdot mg^{-1}$ proteins.

The SOD activity was analyzed by preparing reaction mixtures consisting of enzyme extract, 50 mM extraction buffer (pH 7), 0.13 M methionine, 0.75 mM nitroblue tetrazolium and 0.02 mM riboflavin [41]. The reaction mixtures were illuminated for 15 min (20-W fluorescent tubes), and the sample absorbance recorded at 560 nm was compared with that of the non-illuminated sample that served as a control. One unit (U) of SOD activity was defined as the amount of enzyme required to cause a 50% inhibition of the nitroblue tetrazolium photoreduction rate. The SOD activity was represented as $U \cdot mg^{-1}$ protein.

2.7. Oxidative Stress Marker Contents

The HR extracts for determination of oxidative stress markers H_2O_2 and malondialdehyde (MDA) were prepared from fresh root material using 5% TCA, while the $O_2^{\bullet -}$ production rate was assessed in the same extracts used for antioxidant enzyme activities.

The intracellular H_2O_2 level in HR tissue was determined according to the method of Sergiev et al. [42] that included mixing HR extracts, 10 mM potassium phosphate buffer (pH 7) and 1 M potassium iodide. The absorbance of the samples was measured at 390 nm, and the H_2O_2 content was expressed as micromoles of H_2O_2 equivalents per gram of fresh weight (μM $H_2O_2 \cdot g^{-1}$ FW).

The rate of $O_2^{\bullet -}$ production was measured by preparing a reaction mixture containing HR extract, 50 mM potassium phosphate buffer (pH 7) and 10 mM hydroxylamine hydrochloride [43]. After addition of Griess reagent to the mixture, the sample absorbance was read at 530 nm. The $O_2^{\bullet -}$ production rate in HR was calculated using sodium nitrite as a standard and the results were expressed as nanomoles of generated $O_2^{\bullet -}$ per min and gram of fresh weight (nM $O_2^{\bullet -} \cdot min^{-1} \cdot g^{-1}$ FW).

The MDA content was analyzed by the method of Health and Packer [44]. The HR extracts mixed with 0.5% TBA in 20% TCA were heated at 95 °C for 30 min and then quickly cooled in ice. The sample absorbance was monitored at 532 and 600 nm. After subtracting the non-specific absorbance (600 nm), the MDA contents were calculated using the molar extinction coefficient of MDA (155 $mM^{-1} \cdot cm^{-1}$). The MDA contents were expressed as nanomoles of MDA equivalents per gram of fresh weight (nM MDA$\cdot g^{-1}$ FW).

2.8. Statistical Analysis

The experiments with dark-grown (HR1) and photoperiod-exposed (HR2) clones were repeated independently twice and the analyses were done in triplicate. All data were

presented as an average value with standard deviation (± SD). The data were analyzed by one-way ANOVA (STATISTICA for Windows version 5.0; Tulsa, OK, USA) to detect significant differences between samples. A post hoc separation of means between different clones was performed by the Duncan's multiple range test ($p < 0.05$). Significant differences at $p < 0.05$ between individual HR1 and HR2 clones were determined using the Student's *t*-test. All parameters for phenolic compound contents and antioxidant status were subjected to principal component analysis (PCA) and hierarchical agglomerative clustering (HAC) using the statistical software XLSTAT 2014.5.03 (Addinsoft, NY, USA). The Pearson's correlation coefficients for determination of the relationship between phenolic compound composition and antioxidant status were obtained by R software v. 4.2.1 (R Core Team, Vienna, Austria).

3. Results

3.1. Growth Characteristics of Dark-Grown and Photoperiod-Exposed Hairy Roots

In the present study, phenotypic characteristics and biomass production (FW, DW, FW/DW ratio and DWY) were compared between fifteen dark-grown (HR1 A-HR1 O) and corresponding photoperiod-exposed (HR2 A-HR2 O) clones. Dark-grown HR1 cultures were thinner and whitish in color, showing rapid plagiotropic growth with active branching and vigorous production of elongated lateral roots (Figure 1A). The HR2 cultures also displayed plagiotropic and branching phenotypes, but to a lesser extent compared with HR1. The HR2 cultures were thicker and began to turn pale green after 7 days of culture and continued to acquire a green color during the growth period (Figure 1B).

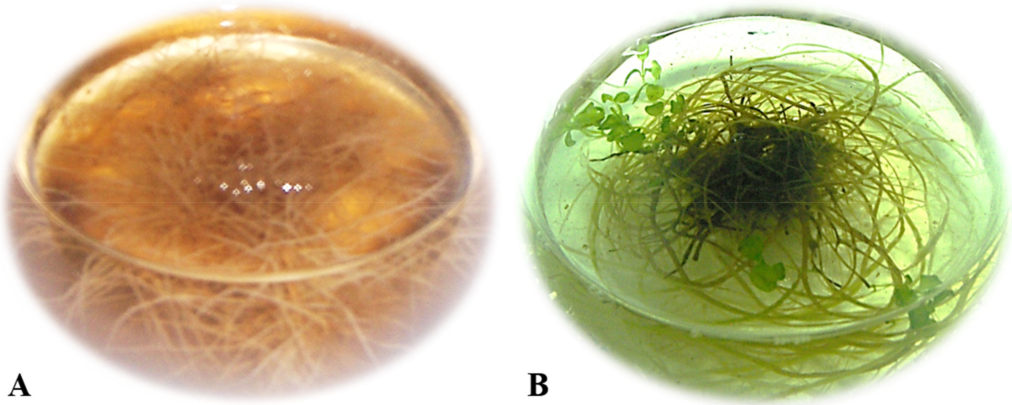

Figure 1. The morphology of *Hypericum perforatum* dark-grown (**A**) and photoperiod-exposed (**B**) transgenic roots.

Outgoing data showed significant differences in growth parameters between HR1 and HR2 cultures (Table 1). The results showed that most of the HR2 clones displayed lower values for FW in comparison with HR1 clones. The exception was found only for HR2 L and HR2 O, which exhibited slightly higher FW accumulation than their corresponding HR1 clones. Similarly, HR2 clones demonstrated lower DW production in comparison with HR1 clones, while only HR2 N had a significantly higher DW production compared with the corresponding dark-grown clone. In general, the FW/DW ratio was not significantly different between most of the HR1 and HR2 clones. Only HR2 D and HR2 M showed a significantly higher FW/DW ratio compared with their corresponding dark-grown clones. With respect to DWY, three photoperiod-exposed clones (HR2 F, HR2 G and HR2 N) showed significantly higher values compared with their corresponding HR1 clones.

Table 1. Growth characteristics of dark-grown and photoperiod-exposed *Hypericum perforatum* hairy roots.

	FW (g)		DW (g)		FW/DW Ratio		DWY	
	HR1	**HR2**	**HR1**	**HR2**	**HR1**	**HR2**	**HR1**	**HR2**
NTR	7.10 ± 0.71^{a}	$2.35 \pm 0.35^{a;*}$	0.56 ± 0.00^{ab}	$0.21 \pm 0.02^{a;*}$	12.72 ± 0.54^{bc}	11.21 ± 0.87^{ab}	$8.26 \pm 0.38^{c–f}$	8.17 ± 0.22^{bh}
A	13.49 ± 0.02^{l}	$7.83 \pm 0.24^{f;*}$	$1.03 \pm 0.01^{e–i}$	$0.61 \pm 0.04^{c;*}$	13.10 ± 1.02^{c}	12.91 ± 0.72^{b}	7.64 ± 0.09^{ae}	8.13 ± 0.70^{bf}
B	18.42 ± 2.09^{m}	16.27 ± 0.24^{j}	1.58 ± 0.12^{j}	1.38 ± 0.09^{h}	$11.69 \pm 0.67^{a–c}$	11.81 ± 1.01^{b}	9.26 ± 0.32^{ef}	8.47 ± 0.68^{bk}
C	12.97 ± 0.80^{kl}	$7.54 \pm 0.48^{d–f;*}$	$1.04 \pm 0.11^{e–i}$	$0.64 \pm 0.06^{c;*}$	$12.44 \pm 0.45^{a–c}$	11.76 ± 0.57^{b}	$8.02 \pm 0.73^{b–f}$	8.52 ± 0.18^{bl}
D	$9.99 \pm 0.64^{d–h}$	$5.21 \pm 0.41^{b;*}$	0.85 ± 0.06^{cdg}	$0.35 \pm 0.03^{b;*}$	$11.79 \pm 0.81^{a–c}$	$14.72 \pm 0.60^{c;*}$	$8.47 \pm 0.44^{d–f}$	$6.79 \pm 0.24^{a;*}$
E	7.71 ± 0.54^{ab}	6.45 ± 0.65^{c}	0.60 ± 0.02^{a}	0.65 ± 0.07^{c}	12.92 ± 0.95^{bc}	$9.96 \pm 0.59^{a;*}$	8.03 ± 0.65^{ac}	$9.10 \pm 0.82^{e–m}$
F	25.66 ± 1.15^{n}	$11.09 \pm 1.00^{i;*}$	1.55 ± 0.14^{j}	$0.90 \pm 0.04^{fg;*}$	16.55 ± 0.40^{e}	$12.28 \pm 1.10^{b;*}$	5.69 ± 0.33^{ab}	$8.16 \pm 0.47^{bg;*}$
G	8.92 ± 0.49^{bce}	$6.85 \pm 0.78^{c;*}$	0.57 ± 0.01^{ac}	0.58 ± 0.02^{c}	15.77 ± 1.10^{de}	$11.88 \pm 0.73^{b;*}$	6.37 ± 0.42^{ad}	$9.00 \pm 0.30^{c–m;*}$
H	10.68 ± 0.27^{gj}	$6.89 \pm 0.55^{cd;*}$	0.86 ± 0.05^{dh}	$0.61 \pm 0.04^{c;*}$	$12.48 \pm 1.31^{a–c}$	11.39 ± 0.48^{b}	$8.00 \pm 0.30^{b–f}$	$8.80 \pm 0.35^{c–m}$
I	$10.38 \pm 0.32^{e–gi}$	$6.93 \pm 0.18^{ce;*}$	0.82 ± 0.04^{cdf}	$0.56 \pm 0.05^{c;*}$	12.71 ± 1.03^{bc}	12.43 ± 0.91^{b}	7.87 ± 0.48^{af}	8.09 ± 0.79^{be}
J	$10.94 \pm 0.17^{h–j}$	$9.05 \pm 0.92^{g;*}$	0.91 ± 0.03^{di}	0.83 ± 0.04^{de}	$12.00 \pm 1.44^{a–c}$	10.86 ± 0.68^{ab}	$8.22 \pm 0.07^{c–f}$	8.29 ± 0.79^{bj}
K	9.13 ± 0.22^{bcf}	$6.35 \pm 0.49^{c;*}$	$0.76 \pm 0.03^{b–d}$	$0.54 \pm 0.05^{c;*}$	$12.08 \pm 1.12^{a–c}$	11.68 ± 1.11^{ab}	$8.28 \pm 0.35^{c–f}$	8.58 ± 0.71^{bm}
L	9.33 ± 0.44^{cg}	$10.76 \pm 0.22^{i;*}$	$0.87 \pm 0.02^{c–e}$	0.87 ± 0.03^{eg}	10.78 ± 0.86^{ab}	12.42 ± 1.20^{b}	$8.69 \pm 0.73^{d–f}$	8.02 ± 018^{bc}
M	$11.80 \pm 1.09^{i–k}$	$9.71 \pm 0.01^{h;*}$	$1.10 \pm 0.05^{e–i}$	$0.78 \pm 0.03^{e;*}$	10.71 ± 0.44^{a}	$12.44 \pm 0.92^{b;*}$	$8.76 \pm 0.28^{d–f}$	8.04 ± 0.34^{bd}
N	8.10 ± 1.27^{ac}	8.55 ± 0.21^{g}	0.54 ± 0.00^{a}	$0.66 \pm 0.03^{cd;*}$	14.87 ± 0.39^{d}	12.96 ± 1.32^{bc}	6.19 ± 0.48^{a}	$7.71 \pm 0.30^{b;*}$
O	$8.61 \pm 0.34^{b–d}$	$10.05 \pm 0.64^{h;*}$	0.77 ± 0.04^{ad}	0.82 ± 0.05^{ef}	$11.20 \pm 0.72^{a–c}$	12.22 ± 1.31^{b}	$8.94 \pm 0.89^{c–f}$	8.19 ± 0.05^{bi}

Note: NTR: control roots; HR1 A-HR1 O: hairy root clones cultured under darkness; HR2 A-HR2 O: hairy root clones cultured under photoperiod; FW: fresh weight; DW: dry weight; FW/DW ratio: fresh weight/dry weight ratio; DWY: dry weight yield. The values in one column marked with different lower-case letters denote significant differences at $p < 0.05$ between clones (Duncan's multiple range test). The values in one row marked with asterisk (*) denote significant differences at $p < 0.05$ between particular HR1 and HR2 clones (Student's *t* test).

3.2. Phenolic Compound Production in Dark-Grown and Photoperiod-Exposed Hairy Roots

The results for TP contents, as well as PAL and PPO activities between HR1 and HR2 clones, are shown in Table 2. The TP contents in HR2 clones were significantly decreased (up to 2-fold) compared with HR1 clones. Concerning PAL as a key enzyme from the phenylpropanoid metabolism, the HR2 clones showed declined activity (from 1.5- to 6.6-fold) compared with the corresponding HR1 clones. The exception was found only for the HR2 I clone, which demonstrated higher PAL activity in comparison with the HR1 I clone. The activity of PPO as the main enzyme involved in the oxidation of phenolics was generally comparable between HR1 and HR2 lines. However, four photoperiod-exposed clones (HR2 E, HR2 F, HR2 H and HR2 N) displayed significantly enhanced PPO activity (up to 2.3-fold) compared with their corresponding HR1 clones.

Table 2. Total phenolic contents, phenylalanine ammonia lyase and polyphenol oxidase activity in dark-grown and photoperiod-exposed *Hypericum perforatum* hairy roots.

	TP (mg GA·g^{-1} DW)		PAL (pkat·mg^{-1} P)		PPO (nkat·mg^{-1} P)	
	HR1	**HR2**	**HR1**	**HR2**	**HR1**	**HR2**
NTR	21.27 ± 0.58 $^{b–d}$	12.86 ± 0.12 $^{a;*}$	1.14 ± 0.14 ^{a}	0.97 ± 0.12 ^{c}	0.14 ± 0.01 ^{df}	0.07 ± 0.01 $^{b;*}$
A	20.80 ± 0.09 ^{ab}	19.76 ± 0.21 ^{h}	1.38 ± 0.35 ^{a}	0.55 ± 0.02 $^{a;*}$	0.17 ± 0.01 ^{h}	0.04 ± 0.00 $^{a;*}$
B	33.19 ± 0.37 ^{k}	23.70 ± 0.61 $^{i;*}$	9.08 ± 0.08 ^{h}	9.25 ± 0.06 ^{h}	0.15 ± 0.01 $^{e–g}$	0.14 ± 0.01 $^{e–i}$
C	21.68 ± 0.36 ^{ce}	17.57 ± 0.09 $^{e;*}$	4.55 ± 0.54 ^{f}	0.98 ± 0.46 $^{c;*}$	0.19 ± 0.02 ^{hi}	0.06 ± 0.00 $^{b;*}$
D	20.42 ± 0.14 ^{a}	19.74 ± 0.55 ^{h}	3.88 ± 0.36 ^{de}	0.59 ± 0.03 $^{a;*}$	0.12 ± 0.00 ^{c}	0.03 ± 0.00 $^{a;*}$
E	24.06 ± 0.33 ^{g}	14.84 ± 0.30 $^{b;*}$	1.48 ± 0.40 ^{a}	1.73 ± 0.50 ^{cd}	0.06 ± 0.01 ^{a}	0.14 ± 0.00 $^{dh;*}$
F	34.82 ± 0.09 ^{l}	24.95 ± 0.28 $^{j;*}$	5.49 ± 0.30 ^{g}	5.94 ± 0.52 ^{g}	0.14 ± 0.01 ^{dg}	0.22 ± 0.03 $^{l;*}$
G	20.99 ± 0.36 ^{ac}	16.82 ± 0.24 $^{d;*}$	3.69 ± 0.24 ^{ce}	1.83 ± 0.01 $^{d;*}$	0.17 ± 0.02 ^{h}	0.16 ± 0.03 ^{j}
H	25.38 ± 0.18 ^{h}	16.41 ± 0.39 $^{d;*}$	3.49 ± 0.32 ^{cd}	4.31 ± 0.50 ^{f}	0.10 ± 0.01 ^{b}	0.16 ± 0.02 $^{j;*}$
I	21.83 ± 0.03 ^{de}	15.14 ± 0.55 $^{bc;*}$	3.30 ± 0.05 ^{c}	4.12 ± 0.04 $^{f;*}$	0.12 ± 0.00 ^{c}	0.13 ± 0.00 ^{de}
J	22.32 ± 0.06 ^{ef}	15.70 ± 0.95 $^{c;*}$	1.58 ± 0.15 ^{a}	1.67 ± 0.43 ^{cd}	0.14 ± 0.01 ^{de}	0.14 ± 0.02 ^{di}
K	23.01 ± 0.54 ^{f}	17.59 ± 0.84 $^{e;*}$	2.36 ± 0.13 ^{b}	1.59 ± 0.54 ^{cd}	0.19 ± 0.03 ^{hj}	0.09 ± 0.00 $^{c;*}$
L	24.88 ± 0.82 ^{h}	18.97 ± 0.18 $^{g;*}$	3.87 ± 0.08 ^{de}	3.12 ± 0.58 ^{e}	0.21 ± 0.01 ^{k}	0.13 ± 0.00 $^{df;*}$
M	31.10 ± 0.30 ^{i}	18.52 ± 0.09 $^{fg;*}$	1.12 ± 0.33 ^{a}	1.62 ± 0.41 ^{cd}	0.13 ± 0.01 ^{cd}	0.12 ± 0.00 ^{d}
N	32.42 ± 1.29 ^{j}	16.64 ± 0.49 $^{d;*}$	1.09 ± 0.00 ^{a}	0.71 ± 0.04 $^{b;*}$	0.09 ± 0.00 ^{b}	0.18 ± 0.01 $^{k;*}$
O	21.89 ± 0.43 ^{de}	17.98 ± 0.30 $^{ef;*}$	2.80 ± 0.57 ^{b}	2.89 ± 0.12 ^{e}	0.19 ± 0.00 ^{ij}	0.13 ± 0.01 $^{dg;*}$

Note: NTR: control roots; HR1 A-HR1 O: hairy root clones cultured under darkness; HR2 A-HR2 O: hairy root clones cultured under photoperiod; TP: total phenolics; PAL: phenylalanine ammonia lyase; PPO: polyphenol oxidase; GA: gallic acid; P: proteins; DW: dry weight. The values in one column marked with different lower-case letters denote significant differences at $p < 0.05$ between clones (Duncan's multiple range test). The values in one row marked with asterisk (*) denote significant differences at $p < 0.05$ between particular HR1 and HR2 clones (Student's *t* test).

The contents of TF, TFA, TA and TH between HR1 and HR2 clones are presented in Table 3. The values for TF and TFA contents in HR2 clones were significantly decreased (up to 3.3-fold) in comparison with those observed for dark-grown clones. Most of the HR2 clones exhibited significantly decreased TA amounts (up to 3-fold) compared with the HR1 clones. The exception was found only for the HR2 A clone as a better producer of TA (1.8-fold) in comparison with its corresponding HR1 A clone. It is interesting to point out that photoperiod-exposed clones showed greater production of TH compared with dark-grown cultures. In this context, seven photoperiod-exposed cultures (HR2 B, HR2 C, HR2 F, HR2 G, HR2 and I-HR2 K) along with NTR2 displayed markedly increased TH amounts (up to 3.4-fold) compared with their corresponding HR1 cultures. Most importantly, HR2 K was shown as a superior clone for TH accumulation compared with the HR1 K clone.

Table 3. Total flavonoids, flavan-3-ols, anthocyanins and hypericins contents in dark-grown and photoperiod-exposed *Hypericum perforatum* hairy roots.

	TF (mg C·g^{-1} DW)		TFA (mg C·g^{-1} DW)		TA (mg CG·g^{-1} DW		TH (μg H·g^{-1} DW)	
	HR1	**HR2**	**HR1**	**HR2**	**HR1**	**HR2**	**HR1**	**HR2**
NTR	7.19 ± 0.26 ^{bg}	3.45 ± 0.11 $^{a;*}$	2.10 ± 0.13 ^{c}	0.72 ± 0.02 $^{a;*}$	1.17 ± 0.01 $^{e–g}$	0.83 ± 0.01 $^{h;*}$	19.54 ± 0.25 ^{c}	62.40 ± 1.01 $^{k;*}$
A	7.15 ± 0.31 ^{bf}	5.47 ± 0.10 $^{e;*}$	1.84 ± 0.01 ^{b}	0.93 ± 0.02 $^{b;*}$	1.09 ± 0.05 ^{de}	1.99 ± 0.00 $^{j;*}$	52.00 ± 0.51 ^{j}	26.36 ± 0.76 $^{d;*}$
B	11.35 ± 0.67 ^{k}	7.04 ± 0.46 $^{g;*}$	5.32 ± 0.00 ^{j}	2.66 ± 0.04 $^{k;*}$	0.78 ± 0.01 ^{b}	0.59 ± 0.07 $^{be;*}$	16.32 ± 0.25 ^{a}	34.25 ± 0.25 $^{f;*}$
C	7.64 ± 0.95 $^{c–h}$	5.11 ± 0.21 $^{e;*}$	2.14 ± 0.10 ^{c}	1.42 ± 0.03 $^{h;*}$	0.96 ± 0.09 ^{c}	0.56 ± 0.03 $^{bc;*}$	26.54 ± 0.51 ^{e}	58.46 ± 1.01 $^{j;*}$
D	7.12 ± 0.57 ^{be}	5.22 ± 0.05 $^{e;*}$	1.63 ± 0.02 ^{a}	1.09 ± 0.12 $^{cd;*}$	1.40 ± 0.01 ^{h}	1.24 ± 0.04 $^{i;*}$	43.75 ± 1.52 ^{h}	42.14 ± 0.76 ^{h}
E	6.82 ± 0.15 ^{b}	4.67 ± 0.33 $^{d;*}$	1.88 ± 0.03 ^{b}	1.06 ± 0.05 $^{c;*}$	0.98 ± 0.17 ^{c}	0.77 ± 0.02 ^{g}	46.98 ± 0.51 ^{i}	19.72 ± 0.51 $^{b;*}$
F	15.15 ± 0.36 ^{l}	7.86 ± 0.47 $^{h;*}$	6.73 ± 0.26 ^{k}	3.83 ± 0.09 $^{l;*}$	0.57 ± 0.01 ^{a}	0.58 ± 0.02 ^{bd}	19.54 ± 0.25 ^{c}	44.47 ± 1.01 $^{i;*}$
G	7.32 ± 0.04 ^{bh}	5.36 ± 0.15 $^{e;*}$	1.85 ± 0.04 ^{b}	1.29 ± 0.02 $^{g;*}$	0.75 ± 0.08 ^{b}	0.70 ± 0.06 ^{f}	26.18 ± 0.51 ^{e}	62.58 ± 1.78 $^{k;*}$
H	8.52 ± 0.29 ^{i}	5.33 ± 0.10 $^{e;*}$	2.82 ± 0.08 ^{h}	1.37 ± 0.02 $^{h;*}$	1.11 ± 0.07 ^{dg}	0.55 ± 0.03 $^{b;*}$	29.41 ± 0.51 ^{f}	24.39 ± 0.51 $^{c;*}$
I	6.17 ± 0.36 ^{a}	4.11 ± 0.22 $^{bc;*}$	2.19 ± 0.08 ^{cd}	1.16 ± 0.03 $^{d–f;*}$	1.61 ± 0.05 ^{j}	0.55 ± 0.04 $^{b;*}$	19.37 ± 0.51 ^{bc}	58.99 ± 1.27 $^{j;*}$
J	5.88 ± 0.26 ^{a}	3.80 ± 0.10 $^{ab;*}$	2.12 ± 0.05 ^{c}	1.13 ± 0.03 $^{ce;*}$	0.97 ± 0.15 ^{c}	0.49 ± 0.04 $^{a;*}$	18.29 ± 0.51 ^{b}	38.55 ± 0.76 $^{g;*}$
K	7.08 ± 0.31 ^{bd}	6.02 ± 0.67 ^{f}	2.48 ± 0.08 ^{f}	1.35 ± 0.01 $^{gh;*}$	1.11 ± 0.01 ^{df}	0.82 ± 0.03 $^{gh;*}$	21.52 ± 0.51 ^{d}	73.34 ± 2.28 $^{l;*}$
L	7.63 ± 0.15 $^{c–h}$	5.16 ± 0.08 $^{e;*}$	2.63 ± 0.01 ^{g}	1.94 ± 0.05 $^{j;*}$	1.05 ± 0.00 ^{cd}	0.62 ± 0.05 $^{c–e;*}$	37.83 ± 0.76 ^{g}	10.22 ± 0.25 $^{a;*}$
M	8.28 ± 0.57 ^{i}	5.33 ± 0.10 $^{e;*}$	4.53 ± 0.16 ^{i}	1.37 ± 0.00 $^{h;*}$	1.16 ± 0.16 $^{e–g}$	1.24 ± 0.05 ^{i}	26.90 ± 1.01 ^{e}	27.26 ± 0.51 ^{d}
N	9.27 ± 0.10 ^{j}	4.27 ± 0.15 $^{c;*}$	2.28 ± 0.07 ^{de}	1.14 ± 0.00 $^{cf;*}$	1.50 ± 0.06 ^{i}	1.23 ± 0.04 $^{i;*}$	55.77 ± 1.27 ^{k}	31.02 ± 0.25 $^{e;*}$
O	7.01 ± 0.62 ^{bc}	5.38 ± 0.08 $^{e;*}$	2.37 ± 0.07 ^{ef}	1.54 ± 0.01 $^{i;*}$	1.17 ± 0.07 $^{e–g}$	1.27 ± 0.03 ^{i}	37.48 ± 1.27 ^{g}	20.08 ± 0.51 $^{b;*}$

Note: NTR: control roots; HR1 A-HR1 O: hairy root clones cultured under darkness; HR2 A-HR2 O: hairy root clones cultured under photoperiod; TF: total flavonoids; TFA: total flavan-3-ols; TA: total anthocyanins; TH: total hypericins; C: catechin; CG: cyanidin-3-glucoside; H: hypericin; DW: dry weight. The values in one column marked with different lower-case letters denote significant differences at $p < 0.05$ between clones (Duncan's multiple range test). The values in one row marked with asterisk (*) denote significant differences at $p < 0.05$ between particular HR1 and HR2 clones (Student's *t* test).

3.3. Non-Enzymatic Antioxidant Activities of Dark-Grown and Photoperiod-Exposed Hairy Roots

Antioxidant activities measured by CUPRAC, DPPH, FCA and LPI assays showed significant differences between HR1 and HR2 lines (Table 4). The CUPRAC and DDPH values for HR2 clones were significantly decreased (up to 2.4-fold) in comparison with HR 1 clones. On the other hand, eight photoperiod-exposed clones (HR2 A-C, HR2 F, HR2 G, HR2 J, HR2 L and HR2 M) including NTR2 displayed significantly enhanced FCA (up to 2.4-fold) compared with HR1 clones. It is worth noting that all HR2 clones displayed exceptionally higher LPI values (up to 4.2-fold) compared with HR1 cultures. The results demonstrate that photoperiod induces antioxidant response in HR2 cultures through the activation of chelation of ferrous ions and inhibition of lipid peroxidation, rather than hydrogen-donating capacity.

3.4. Antioxidant Enzyme Activities of Dark-Grown and Photoperiod-Exposed Hairy Roots

The data demonstrated significant differences in antioxidant enzyme activity (PX, CAT and SOD) between transgenic clones cultured under dark and photoperiod conditions (Table 5). Most of the tested photoperiod-exposed clones (HR2 E-J, HR2 M and HR2 N) displayed significantly enhanced PX activity in comparison with their corresponding HR1 clones. Of note, the HR2 F clone showed a 20-fold increased PX activity compared with its corresponding HR1 F clone. A similar pattern was observed for CAT activity between HR1 and HR2 cultures, since seven photoperiod-exposed lines (HR2 F-I, HR2 K, HR2 N and HR2 O) exhibited markedly enhanced CAT activity (up to 3.3-fold) compared with their corresponding HR1 clones. With respect to SOD activity, six photoperiod-exposed clones (HR2 B, HR2 E, HR2 F, HR2 H, HR2 I and HR2 N) displayed significantly elevated enzyme activity (up to 3.5-fold) compared with the corresponding HR1 clones.

3.5. Oxidative Stress Markers of Dark-Grown and Photoperiod-Exposed Hairy Roots

Oxidative stress marker contents (H_2O_2, $O_2^{\bullet -}$ and MDA) between HR1 and HR2 clones are presented in Table 6. The intracellular H_2O_2 amounts in all tested HR2 clones were significantly decreased compared with the HR1 cultures. The $O_2^{\bullet -}$ production rates in HR2 clones were significantly declined compared with HR1 clones, with the exception of three photoperiod-exposed clones (HR2 A, HR2 D and HR2 E), which showed up to a 2.2-fold enhanced capacity for $O_2^{\bullet -}$ production. The MDA levels in HR2 clones were significantly decreased (up to 2-fold) compared with HR1 clones. However, three photoperiod-exposed clones (HR2 E, HR2 G and HR2 N) showed enhanced MDA amounts (up to 2.2-fold) compared with their corresponding HR1 clones.

3.6. Principal Component Analysis and Hierarchical Agglomerative Clustering

The differences in total contents of phenolic compounds and antioxidant status between *H. perforatum* HR1 and HR2 clones including the NTR cultures were analyzed using principal component analysis (PCA) and hierarchical agglomerative clustering (HAC). These statistical tools of multivariate analysis were performed to determine the variance of phenolic compound contents, PAL and PPO enzyme activities, antioxidant activities, antioxidant enzyme activities and oxidative stress marker contents within HR clones, as well as to cluster the samples depending on analyzed variables (Figure 2).

Table 4. Total antioxidant activities of dark-grown and photoperiod-exposed *Hypericum perforatum* hairy roots *.

	CUPRAC (μM T·g^{-1} DW)		DPPH (μM T·g^{-1} DW)		FCA (mg EDTA·g^{-1} DW)		LPI (%)	
	HR1	**HR2**	**HR1**	**HR2**	**HR1**	**HR2**	**HR1**	**HR2**
NTR	109.58 ± 0.36 ^{b}	69.75 ± 1.97 $^{a;*}$	54.37 ± 0.60 ^{b}	29.48 ± 2.33 $^{a;*}$	3.03 ± 0.21 ^{c}	4.65 ± 0.22 $^{f;*}$	38.90 ± 3.15 ^{egh}	84.23 ± 3.43 $^{fh;*}$
A	101.71 ± 2.30 ^{a}	107.27 ± 1.94 ^{j}	47.75 ± 2.82 ^{a}	50.28 ± 2.79 ^{i}	4.21 ± 0.05 ^{e}	5.67 ± 0.07 $^{h;*}$	47.21 ± 2.28 ^{i}	81.23 ± 5.21 $^{e;*}$
B	171.77 ± 8.90 ^{j}	127.54 ± 0.36 $^{k;*}$	93.03 ± 0.50 ^{j}	60.91 ± 3.68 $^{j;*}$	4.64 ± 0.06 ^{j}	6.56 ± 0.27 $^{i;*}$	27.49 ± 1.70 ^{b}	80.31 ± 2.10 $^{e;*}$
C	130.28 ± 0.12 ^{df}	86.91 ± 2.90 $^{d;*}$	58.38 ± 0.10 ^{c}	47.75 ± 0.40 $^{g–i;*}$	4.35 ± 0.00 ^{eg}	6.61 ± 0.18 $^{i;*}$	36.37 ± 1.01 ^{dfg}	84.20 ± 1.33 $^{fg;*}$
D	118.31 ± 5.20 ^{c}	105.22 ± 0.48 $^{j;*}$	54.72 ± 0.10 ^{b}	45.35 ± 0.60 $^{e–g;*}$	4.26 ± 0.03 ^{ef}	4.25 ± 0.26 ^{de}	18.96 ± 1.96 ^{a}	79.94 ± 1.98 $^{e;*}$
E	152.44 ± 0.24 ^{h}	75.02 ± 1.57 $^{b;*}$	60.07 ± 1.29 ^{ce}	36.20 ± 1.00 $^{b;*}$	3.10 ± 0.19 ^{c}	3.41 ± 0.11 ^{a}	32.81 ± 3.78 ^{cd}	82.53 ± 3.17 $^{ef;*}$
F	212.06 ± 2.06 ^{l}	136.07 ± 6.25 $^{l;*}$	97.18 ± 0.40 ^{k}	68.92 ± 2.82 $^{k;*}$	4.37 ± 0.36 ^{eh}	5.39 ± 0.28 $^{g;*}$	44.29 ± 2.02 ^{hi}	84.39 ± 1.92 $^{fi;*}$
G	126.86 ± 3.27 ^{d}	91.62 ± 0.36 $^{eh;*}$	52.49 ± 0.57 ^{b}	41.83 ± 0.98 $^{c;*}$	2.64 ± 0.07 ^{b}	3.80 ± 0.11 $^{b;*}$	35.89 ± 1.86 ^{de}	90.94 ± 0.04 $^{km;*}$
H	135.96 ± 7.71 ^{fg}	97.95 ± 2.78 $^{i;*}$	61.41 ± 0.80 $^{d–f}$	45.40 ± 1.20 $^{d–fh;*}$	4.42 ± 0.09 ^{ej}	4.11 ± 0.11 ^{cd}	66.17 ± 0.97 ^{k}	88.32 ± 1.14 $^{jk;*}$
I	126.52 ± 0.36 ^{d}	81.27 ± 0.95 $^{c;*}$	60.05 ± 2.96 ^{cd}	38.73 ± 0.20 $^{b;*}$	5.31 ± 0.11 ^{l}	4.48 ± 0.17 $^{ef;*}$	29.36 ± 0.34 ^{bc}	74.84 ± 1.52 $^{d;*}$
J	119.16 ± 3.51 ^{c}	88.96 ± 1.69 $^{de;*}$	53.24 ± 0.20 ^{b}	38.45 ± 1.79 $^{b;*}$	3.64 ± 0.09 ^{d}	5.27 ± 0.26 $^{g;*}$	26.77 ± 2.87 ^{b}	85.84 ± 0.95 $^{g–j;*}$
K	129.51 ± 0.73 ^{de}	94.61 ± 2.66 $^{f–i;*}$	60.21 ± 1.69 ^{cf}	42.68 ± 1.59 $^{cd;*}$	4.39 ± 0.06 ^{ei}	3.88 ± 0.18 $^{bc;*}$	37.77 ± 1.13 ^{ef}	61.74 ± 2.55 $^{b;*}$
L	134.30 ± 1.45 $^{e–g}$	97.12 ± 0.94 $^{i;*}$	69.37 ± 1.29 ^{g}	43.66 ± 1.39 $^{ce;*}$	3.58 ± 0.10 ^{d}	5.39 ± 0.06 $^{g;*}$	28.10 ± 0.34 ^{b}	41.30 ± 2.24 $^{a;*}$
M	165.78 ± 1.69 ^{i}	91.45 ± 4.48 $^{eg;*}$	88.80 ± 4.08 ^{i}	50.28 ± 1.60 $^{i;*}$	2.38 ± 0.02 ^{a}	5.68 ± 0.25 $^{h;*}$	47.86 ± 1.09 ^{i}	71.91 ± 0.69 $^{c;*}$
N	201.88 ± 1.94 ^{k}	90.85 ± 1.69 $^{ef;*}$	96.90 ± 1.99 ^{k}	44.30 ± 0.10 $^{cf;*}$	4.46 ± 0.09 $^{f–j}$	4.37 ± 0.04 ^{e}	40.91 ± 2.22 ^{fh}	89.53 ± 1.31 $^{kl;*}$
O	131.91 ± 2.90 ^{dg}	103.62 ± 2.14 $^{j;*}$	73.80 ± 0.40 ^{h}	49.91 ± 1.14 $^{i;*}$	4.95 ± 0.17 ^{k}	3.85 ± 0.06 $^{b;*}$	54.56 ± 0.71 ^{j}	91.44 ± 0.46 $^{lm;*}$

Note: NTR: control roots; HR1 A-HR1 O: hairy root clones cultured under darkness; HR2 A-HR2 O: hairy root clones cultured under photoperiod; CUPRAC: cupric ions reducing antioxidant capacity; DPPH: 2,2-diphenyl-1-picrylhydrazyl radical scavenging; FCA: ferrous chelating activity; LPI: lipid peroxidation inhibition; T: trolox; EDTA: ethylenediaminetetraacetic acid; DW: dry weight. The values in one column marked with different lower-cases denote significant differences at $p < 0.05$ between clones (Duncan's multiple range test). The values in one row marked with asterisk (*) denote significant differences at $p < 0.05$ between particular HR1 and HR2 clones (Student's *t* test).

Table 5. Antioxidant enzyme activities in dark-grown and photoperiod-exposed *Hypericum perforatum* hairy roots.

	PX (nkat·mg^{-1} P)		CAT (nkat·mg^{-1} P)		SOD (U·mg^{-1})	
	HR1	**HR2**	**HR1**	**HR2**	**HR1**	**HR2**
NTR	1.24 ± 0.02 ^{m}	0.78 ± 0.20 $^{de;*}$	1.24 ± 0.21 ^{c}	1.36 ± 0.06 ^{bc}	13.87 ± 0.76 ^{deg}	6.89 ± 1.08 $^{c;*}$
A	0.94 ± 0.08 ^{hik}	0.35 ± 0.01 $^{b;*}$	4.65 ± 0.18 ^{h}	0.33 ± 0.04 $^{a;*}$	18.66 ± 1.60 ^{h}	5.27 ± 0.19 $^{b;*}$
B	0.22 ± 0.06 ^{b}	0.05 ± 0.01 $^{a;*}$	11.56 ± 0.03 ^{k}	3.35 ± 0.00 $^{ef;*}$	18.52 ± 1.60 ^{h}	22.10 ± 0.62 $^{j;*}$
C	0.88 ± 0.13 ^{gil}	0.51 ± 0.02 $^{bc;*}$	3.19 ± 0.06 ^{i}	1.70 ± 0.10 $^{c;*}$	20.90 ± 1.94 ^{i}	8.39 ± 0.22 $^{d;*}$
D	0.49 ± 0.01 ^{ef}	0.09 ± 0.00 $^{a;*}$	1.03 ± 0.03 ^{a}	0.18 ± 0.01 $^{a;*}$	12.37 ± 0.36 ^{ce}	2.55 ± 0.28 $^{a;*}$
E	0.58 ± 0.06 ^{f}	0.84 ± 0.06 $^{eh;*}$	2.24 ± 0.09 ^{e}	1.69 ± 0.12 $^{c;*}$	4.58 ± 0.46 ^{a}	16.08 ± 0.00 $^{g–i;*}$
F	0.07 ± 0.04 ^{a}	1.45 ± 0.01 $^{j;*}$	2.60 ± 0.04 ^{g}	8.54 ± 0.80 $^{k;*}$	20.20 ± 1.70 ^{hi}	25.63 ± 0.56 $^{l;*}$
G	0.36 ± 0.00 $^{c–e}$	2.39 ± 0.14 $^{k;*}$	5.55 ± 0.08 ^{j}	7.50 ± 0.29 $^{j;*}$	21.28 ± 2.35 ^{i}	24.30 ± 2.00 ^{k}
H	0.56 ± 0.09 ^{f}	1.33 ± 0.00 $^{j;*}$	1.06 ± 0.07 ^{ab}	3.14 ± 0.02 $^{e;*}$	10.82 ± 0.43 ^{c}	22.95 ± 1.83 $^{j;*}$
I	0.82 ± 0.08 ^{gh}	1.06 ± 0.02 $^{i;*}$	1.21 ± 0.13 ^{bc}	3.51 ± 0.17 $^{f;*}$	12.06 ± 0.60 ^{cd}	15.60 ± 0.66 $^{fi;*}$
J	0.54 ± 0.00 ^{f}	0.70 ± 0.07 $^{ce;*}$	2.24 ± 0.03 ^{e}	1.27 ± 0.28 $^{b;*}$	15.66 ± 1.96 ^{g}	15.82 ± 0.13 $^{g–i}$
K	0.76 ± 0.01 ^{g}	0.59 ± 0.01 $^{cd;*}$	1.98 ± 0.20 ^{d}	3.94 ± 0.07 $^{g;*}$	14.73 ± 1.70 ^{fg}	10.53 ± 0.16 $^{e;*}$
L	0.93 ± 0.08 $^{h–j}$	1.01 ± 0.22 $^{f–i}$	2.62 ± 0.07 ^{g}	2.43 ± 0.06 ^{d}	23.45 ± 0.74 ^{j}	14.80 ± 1.35 $^{fg;*}$
M	0.30 ± 0.11 ^{bc}	1.28 ± 0.06 $^{j;*}$	2.51 ± 0.12 ^{fg}	2.37 ± 0.06 ^{d}	13.12 ± 0.25 $^{d–f}$	14.34 ± 0.26 ^{f}
N	0.31 ± 0.05 ^{bd}	0.83 ± 0.09 $^{eg;*}$	3.21 ± 0.30 ^{i}	5.33 ± 0.63 $^{h;*}$	8.43 ± 0.04 ^{b}	15.78 ± 1.04 $^{g–i;*}$
O	0.98 ± 0.11 $^{j–l}$	0.81 ± 0.13 ^{ef}	2.38 ± 0.08 ^{ef}	6.79 ± 0.40 $^{i;*}$	18.52 ± 0.36 ^{h}	15.04 ± 0.69 $^{fh;*}$

Note: NTR: control roots; HR1 A-HR1 O: hairy root clones cultured under darkness; HR2 A-HR2 O: hairy root clones cultured under photoperiod; PX: guaiacol peroxidase; CAT: catalase; SOD: superoxide dismutase; P: proteins. The values in one column marked with different lower-case letters denote significant differences at $p < 0.05$ between clones (Duncan's multiple range test). The values in one row marked with asterisk (*) denote significant differences at $p < 0.05$ between particular HR1 and HR2 clones (Student's *t* test).

Table 6. Oxidative stress marker contents in dark-grown and photoperiod-exposed *Hypericum perforatum* hairy roots.

	H_2O_2 (μM·g^{-1} FW)		$O_2^{\bullet-}$ (nM·min^{-1}·g^{-1} FW)		MDA (nM·g^{-1} FW)	
	HR1	**HR2**	**HR1**	**HR2**	**HR1**	**HR2**
NTR	0.51 ± 0.00 ^{h}	0.79 ± 0.08 $^{l;*}$	0.24 ± 0.01 ^{h}	0.84 ± 0.01 $^{k;*}$	0.66 ± 0.00 ^{ce}	0.39 ± 0.05 $^{a;*}$
A	0.37 ± 0.05 ^{b}	0.47 ± 0.04 $^{j;}$	0.14 ± 0.00 ^{b}	0.26 ± 0.05 $^{i;*}$	0.63 ± 0.01 ^{cd}	0.55 ± 0.05 ^{be}
B	0.41 ± 0.02 $^{c–g}$	0.20 ± 0.00 $^{a;*}$	0.28 ± 0.01 ^{j}	0.09 ± 0.00 $^{a;*}$	1.42 ± 0.01 ^{k}	1.14 ± 0.06 $^{l;*}$
C	0.56 ± 0.03 ^{i}	0.45 ± 0.01 $^{ij;*}$	0.21 ± 0.03 ^{d}	0.20 ± 0.01 $^{c–f}$	0.94 ± 0.03 ^{i}	0.58 ± 0.00 $^{c–f;*}$
D	0.49 ± 0.04 ^{h}	0.54 ± 0.01 ^{k}	0.22 ± 0.00 ^{dg}	0.48 ± 0.05 $^{j;*}$	0.68 ± 0.02 $^{d–f}$	0.56 ± 0.04 $^{c–e;*}$
E	0.65 ± 0.05 ^{j}	0.44 ± 0.03 $^{i;*}$	0.19 ± 0.00 ^{c}	0.25 ± 0.00 $^{g–i;*}$	0.44 ± 0.01 ^{b}	0.98 ± 0.00 $^{k;*}$
F	0.32 ± 0.04 ^{a}	0.27 ± 0.01 ^{b}	0.26 ± 0.00 ^{i}	0.11 ± 0.01 $^{a;*}$	1.05 ± 0.05 ^{j}	0.72 ± 0.00 $^{i;*}$
G	0.50 ± 0.01 ^{h}	0.29 ± 0.03 $^{bf;*}$	0.22 ± 0.01 ^{df}	0.11 ± 0.01 $^{a;*}$	0.43 ± 0.04 ^{b}	0.85 ± 0.14 $^{j;*}$
H	0.43 ± 0.00 ^{g}	0.31 ± 0.00 $^{c–g;*}$	0.21 ± 0.01 ^{de}	0.23 ± 0.01 ^{fg}	0.94 ± 0.09 ^{i}	0.49 ± 0.01 $^{b;*}$
I	0.37 ± 0.01 ^{bc}	0.30 ± 0.01 $^{bg;*}$	0.28 ± 0.00 ^{j}	0.17 ± 0.01 $^{bd;*}$	0.81 ± 0.03 ^{h}	0.60 ± 0.01 $^{eh;*}$
J	0.39 ± 0.01 ^{bf}	0.32 ± 0.00 $^{e–g;*}$	0.12 ± 0.00 ^{a}	0.15 ± 0.01 ^{b}	0.72 ± 0.04 ^{fg}	0.54 ± 0.01 $^{bd;*}$
K	0.38 ± 0.04 ^{bd}	0.36 ± 0.04 ^{h}	0.30 ± 0.01 ^{k}	0.23 ± 0.01 $^{fh;*}$	0.61 ± 0.07 ^{c}	0.50 ± 0.02 ^{b}
L	0.43 ± 0.02 ^{g}	0.27 ± 0.01 $^{bc;*}$	0.23 ± 0.01 $^{e–g}$	0.17 ± 0.03 ^{bc}	0.69 ± 0.00 ^{eg}	0.74 ± 0.03 ^{i}
M	0.38 ± 0.00 ^{be}	0.29 ± 0.01 $^{be;*}$	0.34 ± 0.01 ^{l}	0.23 ± 0.00 $^{fi;*}$	1.03 ± 0.03 ^{j}	0.62 ± 0.01 $^{fh;*}$
N	0.51 ± 0.05 ^{h}	0.28 ± 0.04 $^{bd;*}$	0.25 ± 0.01 ^{hi}	0.24 ± 0.02 $^{g–i}$	0.34 ± 0.02 ^{a}	0.54 ± 0.03 $^{bc;*}$
O	0.44 ± 0.01 ^{g}	0.23 ± 0.01 $^{a;*}$	0.26 ± 0.01 ^{i}	0.17 ± 0.00 $^{be;*}$	0.73 ± 0.09 ^{fg}	0.81 ± 0.04 ^{j}

Note: NTR: control roots; HR1 A-HR1 O: hairy root clones cultured under darkness; HR2 A-HR2 O: hairy root clones cultured under photoperiod; H_2O_2: hydrogen peroxide; $O_2^{\bullet-}$: superoxide anion; MDA: malondialdehyde; FW: fresh weight. The values in one column marked with different lower-case letters denote significant differences at $p < 0.05$ between clones (Duncan's multiple range test). The values in one row marked with asterisk (*) denote significant differences at $p < 0.05$ between particular HR1 and HR2 clones (Student's *t* test).

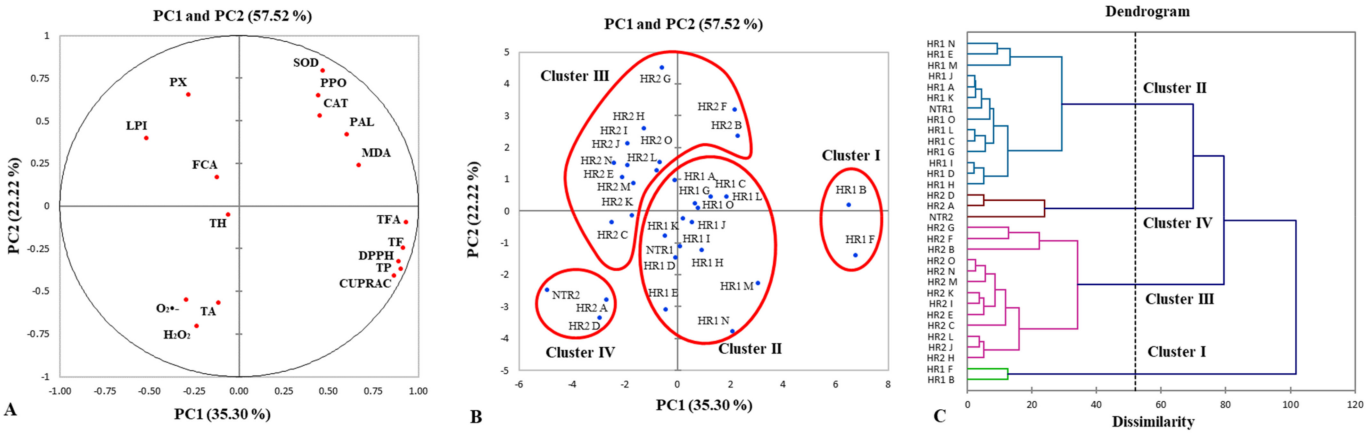

Figure 2. Loadings plot (**A**) and scores plot (**B**) of principal component analysis and hierarchical agglomerative clustering (**C**) for phenolic compound production and antioxidant status of dark-grown and photoperiod-exposed *Hypericum perforatum* hairy roots. PC: principal components; Note: NTR: control roots; HR1 A-HR1 O: hairy root clones cultured under darkness; HR2 A-HR2 O: hairy root clones cultured under photoperiod; TP: total phenolics; TF: total flavonoids; TFA: total flavan-3-ols; TA: total anthocyanins; TH: total hypericins; CUPRAC: cupric reducing antioxidant capacity; DPPH: DPPH radical scavenging activity; FCA: ferrous chelating activity; LPI: lipid peroxidation inhibition; PAL: phenylalanine ammonia lyase; PPO: polyphenol oxidase; PX: guaiacol peroxidase; CAT: catalase; SOD: superoxide dismutase; H_2O_2: hydrogen peroxide; $O_2^{\bullet -}$: superoxide anion; MDA: malondialdehyde.

Two PC were used to characterize phenolic compound composition and antioxidant status of tested HR cultures. The PCA data showed that PC1 and PC2 explained 57.52% of the total variation. The loadings plot of PCA (Figure 2A) indicated that PC1 explained the variance of 35.30% that was positively related to the phenolic compound production (TP, TF and TFA), PAL activity, antioxidant activities (CUPRAC and DPPH) and MDA content of analyzed samples. In contrast, the PC1 was negatively related only with the antioxidant activity measured by LPI. The PC2 showed a variance of 22.22% and it was positively related to the antioxidant enzyme activities (PX, CAT and SOD), as well as to PPO activity, but negatively connected to TA production and oxidative stress marker contents (H_2O_2 and $O_2^{\bullet -}$).

The results for phenolic compound contents and antioxidant status showed that the control and HR cultures were separated on PC1 and PC2 (Figure 2B) and grouped into four clusters (Figure 2C). Cluster I was represented with only two dark-grown clones (HR1 B and HR1 F) with the largest positive score on PC1. Those clones were described with intensive phenylpropanoid metabolism that resulted in accumulation of phenolic compounds with hydrogen-donating capacity. Cluster II included all remaining dark-grown HR1 clones, including NTR1, with positive scores on PC1 that were characterized by moderate production of phenolic compounds with antioxidant activities. Cluster III included almost all photoperiod-exposed HR2 clones with negative scores on PC1 that were characterized by low production of phenolic compounds, but a higher capacity for inhibition of lipid peroxidation, resulting in low accumulation of MDA. The exception was found only for two photoperiod-exposed clones (HR2 B and HR2 F), which showed positive scores on PC1 and resembled the characteristics of dark-grown HR1 clones. In addition, HR2 clones were characterized with positive scores on PC2, indicating their strong enzymatic antioxidant activity, which resulted in suppression of oxidative stress marker contents. Cluster IV included only two photoperiod-exposed HR2 clones (HR2 A and HR2 D), as well as the control roots (NTR2), which were represented by the lowest capacity for the production of phenolics and decreased antioxidant status, causing significant accumulation of oxidative stress markers.

According to the Pearson's correlation matrix (Figure 3), several groups of phenolic compounds (TP, TF and TFA) showed significant positive correlations with antioxidant activity (CUPRAC and DPPH), as well as with the MDA accumulation. On the other hand, TP and TF exhibited significant negative correlations with the LPI and PX activity. The PAL activity showed a significant positive correlation with TF, TFA and MDA levels, while PPO activity showed a significant negative correlation with H_2O_2 and $O_2^{\bullet -}$ amounts. Both PAL and PPO enzyme activities demonstrated positive correlations with antioxidant enzyme activities (CAT and SOD). Concerning the antioxidant enzymes, the PX activity showed a significant negative correlation with TP and TF, as well as with CUPRAC and DPPH. Significant positive correlations were observed between all tested antioxidant enzyme parameters. The H_2O_2 and $O_2^{\bullet -}$ levels expressed significant negative correlations with CAT and SOD activities. It is interesting to point out that the MDA amount showed a significant positive correlation with phenolics (TP, TF and TFA) and DPPH activity, as well as with PAL, CAT and SOD enzyme activities.

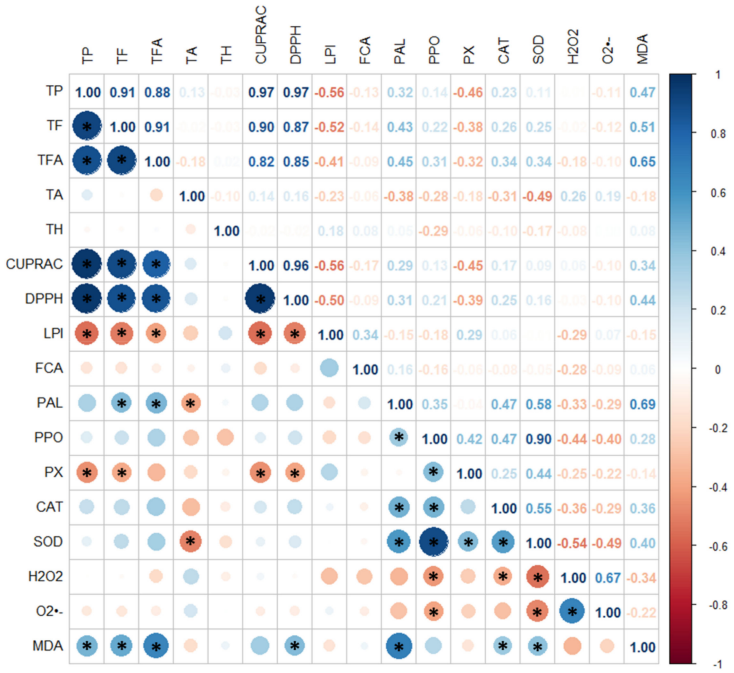

Figure 3. Correlation matrix between phenolic compound production and antioxidant status of dark-grown and photoperiod-exposed *Hypericum perforatum* hairy roots. Black asterisks indicate the significance of the correlation ($p < 0.05$). Blue colors indicate positive correlation, while red colors indicate negative correlation. TP: total phenolics; TF: total flavonoids; TFA: total flavan-3-ols; TA: total anthocyanins; TH: total hypericins; CUPRAC: cupric reducing antioxidant capacity; DPPH: DPPH radical scavenging activity; FCA: ferrous chelating activity; LPI: lipid peroxidation inhibition; PAL: phenylalanine ammonia lyase; PPO: polyphenol oxidase; PX: guaiacol peroxidase; CAT: catalase; SOD: superoxide dismutase; H_2O_2: hydrogen peroxide; $O_2^{\bullet -}$: superoxide anion; MDA: malondialdehyde.

4. Discussion

4.1. Growth Characteristics of Dark-Grown and Photoperiod-Exposed Hairy Roots

In this study, *H. perforatum* dark-grown (HR1 A-HR1 O) and photoperiod-exposed (HR2 A-HR2 O) transgenic roots were cultured in liquid medium to evaluate biomass accumulation and secondary metabolites production. Liquid-grown HR clones displayed exceptionally better growth performance in comparison with previously reported data for *H. perforatum* HR clones cultured on solid medium [25]. One explanation for significant biomass accumulation of liquid-grown transgenic roots could be represented by the fast uptake of exogenously applied nutrients in the medium, such as sucrose, nitrate, am-

monium and other minerals. Another could be the intensive plagiotropic growth of HR clones, which increases the aeration in liquid medium leading to an elevated production of root biomass.

Dark-grown HR1 clones were thinner and whitish in color, with high biomass accumulation compared with photoperiod-exposed HR2 clones that were thicker and green with spontaneous capacity for shoot regeneration. We have previously reported such morphological traits and decreased biomass production in light-exposed *H. perforatum* HR [28]. The main reason for the photoperiod-inhibitory effect on the growth of HR cells could be related to the antagonistic relationship between light and endogenous auxin concentrations [45]. Since extensive proliferation of HR depends on auxin autotrophy, the light exposure is likely to cause oxidation of intrinsic auxins, resulting in declined HR growth. It has already been shown that light interferes with exogenously applied auxins in the medium that slow down the growth of *H. perforatum* adventitious roots [13]. To the best of our knowledge, dark-grown HR cultures use the carbon and energy sources from nutrient medium exclusively for mass root proliferation. On the other hand, light-irradiation-induced chlorophyll biosynthesis in HR cultures leads to the accumulation of photosynthetically-derived carbohydrates [46]. Since the photoperiod-exposed HR2 clones evaluated in this study exhibited regenerative potential, their growth was probably related to the usage of photosynthetic assimilates for shoot organogenesis, rather than for root proliferation. In contrast to these observations, the stimulatory effect of light on HR growth has been confirmed in *Ageratum conyzoides* L. [45] and *Ipomoea aquatica* Forsk. [47]. Even those studies revealed light-dependent root growth; the physiological mechanisms of intensive HR development upon light exposure still remain unknown.

The growth performance of *H. perforatum* HR1 and HR2 cultures was also evaluated through determination of the FW/DW ratio as an index of cell water content and DWY as an indicator for biosynthetic capacity. Photoperiod-exposed HR2 clones showed similar or lower FW/DW values compared with dark-grown HR1 cultures. The root biomass increment through cell division and elongation depends on water uptake [48]. Taking this into account, the slow growth of the photoperiod-exposed HR2 clones could be related to the low water uptake from the nutrient medium, resulting in decreased water content in root cells. Despite the limited fresh biomass accumulation, the photoperiod-exposed HR2 cultures exhibited comparable or even higher DWY values than the dark-grown HR1 clones. The elevation of DWY in the photoperiod-exposed HR2 clones indicates that light might induce some stress responses in root cells, leading to the activation of secondary metabolite pathways.

4.2. Phenolic Compound Composition of Dark-Grown and Photoperiod-Exposed Hairy Roots

Photoperiod-exposed *H. perforatum* HR2 cultures accumulated lower contents of phenolics, flavonoids and flavan-3-ols compared with dark-grown HR1 clones. It has already been reported that light exposure inhibits the production of phenolic compounds in HR cultures by enhancement of the metabolic flux out of the secondary metabolite pool [29,49]. Despite the fact that continuous light irradiation of HR cultures has a major influence on anthocyanin production [50], the cultivation of HR2 clones under photoperiod in this study was not a sufficiently strong stimulus to trigger anthocyanin biosynthesis. Our data indicated that light as a physical stimulus inhibited PAL activity in photoperiod-exposed HR2 clones, which was in correlation with reduced production of phenolics and flavonoids. Similar results have been observed for green HR cultures of *Daucus carota* L., where phenolics generated upon light irradiation have been involved in feedback inhibition of PAL activity [29]. The regulation of PAL activity is complex due to the existence of multiple encoding genes that could be expressed in specific tissues, depending on developmental stage or environmental stimuli [51].

It is worth pointing out that the photoperiod-exposed HR2 cultures were shown as better producers of hypericins compared with the dark-grown HR1 clones. The enhancement of hypericins in HR2 clones could be related to the possible light-dependent formation

of glandular structures for naphthodianthrone accumulation in root tissues. In this view, *H. perforatum* adventitious roots have been proposed as an alternative source for hypericin production due to development of dark red globules on the root tips [52]. Since hypericin could be synthesized in mesophyll, root or stem cells, and transported to the dark glands on leaf margins [53], the shoot organogenic potential of HR2 clones may be, at least in part, responsible for naphthodianthrone production. In addition, *H. perforatum* adventitious roots exposed to red light showed shoot regenerative potential and enhanced hypericin production [13]. These observations indicate that light exposition might trigger some signaling pathways in *H. perforatum* HR that could induce shifting of the phenylpropanoid/flavonoid pathways toward naphthodianthrone biosynthesis.

Unlike PAL as the key enzyme in phenylpropanoid biosynthesis, the PPO is responsible for oxidation of phenolic compounds into quinones [54]. The declining PPO activity in photoperiod-exposed HR2 clones could be attributed to the enzyme photoinactivation followed by conformational modification of its active site, leading to the reduction of cupric ions, which are essential for oxidation processes [55]. These findings reveal that darkness seems to be necessary for PAL and PPO activities in phenylpropanoid/flavonoid metabolism in HR clones. Further insights into light-dependent biosynthesis of secondary metabolites would be desirable to reveal the coordination of phenylpropanoid/flavonoid and naphthodianthrone pathways in *H. perforatum* HR cultures.

4.3. Non-Enzymatic Antioxidant Activities in Dark-Grown and Photoperiod-Exposed Hairy Roots

The dark-grown HR1 clones showed superior hydrogen-donating capability through CUPRAC and DPPH assays, while photoperiod-exposed HR2 were selected as better chelators of ferrous ions and inhibitors of lipid peroxidation. Flavonoids and flavan-3-ols contents in HR clones displayed significant a positive correlation with CUPRAC and DPPH antioxidant capacities. These results were expected since phenolics and flavonoids possess ideal chemical structures for electron or hydrogen donation. In accordance, we have previously confirmed the contribution of phenolic compounds to the antioxidant activity of *H. perforatum* HR transformed with *A. rhizogenes* strains A4M70GUS [24] and A4 [25]. The enhanced FCA and LPI properties in photoperiod-exposed HR2 clones might be related to the elevated accumulation of hypericins. A positive correlation observed between LPI and hypericin contents indicated that the β-carotene bleaching assay could be considered as a suitable method for determination of hydrophobic antioxidants. All these observations suggest that photoperiod induces a strong diversification of the redox system in HR2 clones, resulting in the accumulation of hypericins as lipophilic antioxidants.

4.4. Antioxidant Enzymes and Oxidative Stress Markers in Dark-Grown and Photoperiod-Exposed Hairy Roots

It is well known that the activation of antioxidant enzymes in response to photooxidative stress plays a crucial role in the protection of plant cells against excessive ROS production [56]. The evaluation of the enzymatic antioxidant system in *H. perforatum* HR2 clones in response to photoperiod revealed an up-regulation of antioxidant enzymes (SOD, CAT and PX) that resulted in suppression of oxidative stress markers (H_2O_2 and $O_2^{\bullet -}$). The SOD is represented with different isoforms of metalloenzymes acting as the first defense line against oxidative stress through dismutation of highly reactive superoxide anions into H_2O_2 and O_2 [56]. The enhanced SOD activity in the photoperiod-exposed HR2 clones was related to declining $O_2^{\bullet -}$ production and intracellular levels of H_2O_2, indicating its active involvement in photoprotection of root tissues. Catalase converts H_2O_2 to H_2O and O_2 molecules and it is considered as an essential antioxidant enzyme for detoxification of ROS in plant cells [56]. Our results demonstrated that elevation of CAT activity significantly contributed to the decreasing of H_2O_2 contents in photoperiod-exposed HR2 clones. In contrast, light-dependent inactivation of CAT as a photosensitive enzyme has been observed in green HR of *D. carota* exposed to continuous light [29]. As presently established, the exposure of HR2 to photoperiod up-regulated CAT activity, since the dark

regime of 8 h used here probably prevented this enzyme from photodegradation. It is worth noting that the significant positive correlation between SOD and CAT in tested HR cultures might be ascribed to the fact that both enzymes share substrates and products. Moreover, the CAT enzyme showed a better capacity for H_2O_2 reduction in comparison with PX. It is well known that PX reduces H_2O_2 to H_2O by using guaiacol as an aromatic electron donor, and its activity has an important role in defense responses against abiotic and biotic factors [56]. Despite the up-regulation of PX in photoperiod-exposed HR2 clones, the significant contribution of this antioxidant enzyme to intracellular H_2O_2 levels was not found. All these observations suggested that CAT rather than PX was dominantly involved in H_2O_2 scavenging in root cells and protection from light-mediated oxidative stress. Similar results have been reported for PX and SOD activities in *Ipomoea aquatica* HR upon light exposure [46,57]. These authors showed that antioxidant enzymes significantly correlated with development of thylakoid membranes and chlorophyll biosynthesis in green HR cultures. Taking this into account, the presence of chloroplasts in root cells might be responsible for activation of the antioxidant enzyme system in photoperiod-exposed *H. perforatum* HR2 clones.

In this study, MDA levels were used as a biomarker for oxidative stress and potential lipid peroxidation in *H. perforatum* HR2 clones cultured under photoperiod. The declining MDA levels in HR2 clones coincided with low levels of H_2O_2 and $O_2^{\bullet -}$ production. These findings indicate that the activation of the antioxidant enzymatic system in HR2 cultures might suppress lipid peroxidation upon photooxidative stress. On the other hand, results from our previous study showed a positive correlation between MDA levels and antioxidant status of *H. perforatum* solid-grown HR cultured under darkness [25]. These data indicate that *A. rhizogenes*-mediated transformation triggers lipid peroxidation processes in HR cells. Therefore, it could be considered that photoperiod exposition is likely to be involved in the protection of HR2 cells from amelioration processes induced by lipid peroxidation.

5. Conclusions

This is the first study for the evaluation of non-enzymatic and enzymatic antioxidant responses of fifteen *Hypericum perforatum* L. dark-grown (HR1 A-HR1 O) and photoperiod-exposed (HR2 A-HR2 O) hairy root clones. The growth inhibition of photoperiod-exposed HR2 clones was related to their regenerative potential and usage of photosynthetic assimilates for shoot organogenesis. These cultures grown under photoperiod were proposed as an alternative source for accumulation of hypericins as lipophilic antioxidants. On the other hand, dark-grown HR1 clones represented an efficient system for production of flavonoids, flavan-3-ols and anthocyanins, with a strong hydrogen-donating capacity. The up-regulation of antioxidant enzymatic systems in HR2 cultures suppressed photooxidative stress and lipid peroxidation processes. Further studies will be focused on the regeneration of *H. perforatum* hairy roots into transgenic plants as a novel biotechnological tool for evaluation of naphthodianthrones as biological active compounds.

Author Contributions: Conceptualization, methodology, validation, formal analysis, investigation, software, resources, data curation, visualization, writing—review and editing, O.T. and S.G.S.; writing—original draft preparation, O.T.; supervision, S.G.S. All authors have read and agreed to the published version of the manuscript.

Funding: This research received no external funding.

Institutional Review Board Statement: Not applicable.

Informed Consent Statement: Not applicable.

Data Availability Statement: The presented data in this study are available on request from the corresponding author.

Conflicts of Interest: The authors declare no conflict of interest.

References

1. Velingkar, V.S.; Gupta, G.L.; Hegde, N.B. A current update on phytochemistry, pharmacology and herb–drug interactions of *Hypericum perforatum*. *Phytochem. Rev.* **2017**, *16*, 725–744. [CrossRef]
2. Murch, S.J.; Saxena, P.K. St. John's wort (*Hypericum perforatum* L.): Challenges and strategies for production of chemically-consistent plants. *Can. J. Plant Sci.* **2006**, *86*, 765–771. [CrossRef]
3. Kuo, C.-H.; Chou, Y.-C.; Liao, K.-C.; Shieh, C.-J.; Deng, T.-S. Optimization of Light Intensity, Temperature, and Nutrients to Enhance the Bioactive Content of Hyperforin and Rutin in St. John's Wort. *Molecules* **2020**, *25*, 4256. [CrossRef] [PubMed]
4. Mir, M.Y.; Hamid, S.; Kamili, A.N.; Hassan, Q.P. Sneak peek of *Hypericum perforatum* L.: Phytochemistry, phytochemical efficacy and biotechnological interventions. *J. Plant Biochem. Biotechnol.* **2019**, *28*, 357–373. [CrossRef]
5. Gadzovska, S.; Maury, S.; Ounnar, S.; Righezza, M.; Kascakova, S.; Refregiers, M.; Spasenoski, M.; Joseph, C.; Hagège, D. Identification and quantification of hypericin and pseudohypericin in different *Hypericum perforatum* L. in vitro cultures. *Plant Physiol. Biochem.* **2005**, *43*, 591–601. [CrossRef] [PubMed]
6. Gadzovska, S.; Maury, S.; Delaunay, A.; Spasenoski, M.; Hagège, D.; Courtois, D.; Joseph, C. The influence of salicylic acid elicitation of shoots, callus, and cell suspension cultures on production of naphtodianthrones and phenylpropanoids in *Hypericum perforatum* L. *Plant Cell Tissue Organ Cult.* **2012**, *113*, 25–39. [CrossRef]
7. Liu, X.-N.; Zhang, X.-Q.; Sun, J.-S. Effects of cytokinins and elicitors on the production of hypericins and hyperforin metabolites in Hypericum sampsonii and *Hypericum perforatum*. *Plant Growth Regul.* **2007**, *53*, 207–214. [CrossRef]
8. Kwiecień, I.; Smolin, J.; Beerhues, L.; Ekiert, H. The impact of media composition on production of flavonoids in agitated shoot cultures of the three *Hypericum perforatum* L. cultivars 'Elixir,' 'Helos,' and 'Topas'. *Vitr. Cell Dev. Biol. Plant* **2018**, *54*, 332–340. [CrossRef]
9. Tusevski, O.; Stanoeva, J.P.; Markoska, E.; Brndevska, N.; Stefova, M.; Simic, S.G. Callus cultures of *Hypericum perforatum* L. a novel and efficient source for xanthone production. *Plant Cell Tissue Organ Cult.* **2016**, *125*, 309–319. [CrossRef]
10. Cui, X.-H.; Chakrabarty, D.; Lee, E.-J.; Paek, K.-Y. Production of adventitious roots and secondary metabolites by *Hypericum perforatum* L. in a bioreactor. *Bioresour. Technol.* **2010**, *101*, 4708–4716. [CrossRef]
11. Tocci, N.; Simonetti, G.; D'Auria, F.D.; Panella, S.; Palamara, A.T.; Valletta, A.; Pasqua, G. Root cultures of *Hypericum perforatum* subsp. angustifolium elicited with chitosan and production of xanthone-rich extracts with antifungal activity. *Appl. Microbiol. Biotechnol.* **2011**, *91*, 977–987. [CrossRef] [PubMed]
12. Brasili, E.; Miccheli, A.; Marini, F.; Praticò, G.; Sciubba, F.; Di Cocco, M.E.; Cechinel, V.F.; Tocci, N.; Valletta, A.; Pasqua, G. Metabolic Profile and Root Development of *Hypericum perforatum* L. In vitro Roots under Stress Conditions Due to Chitosan Treatment and Culture Time. *Front. Plant Sci.* **2016**, *7*, 507. [CrossRef] [PubMed]
13. Najafabadi, A.S.; Khanahmadi, M.; Ebrahimi, M.; Moradi, K.; Behroozi, P.; Noormohammadi, N. Effect of different quality of light on growth and production of secondary metabolites in adventitious root cultivation of *Hypericum perforatum*. *Plant Signal. Behav.* **2019**, *14*, 1640561. [CrossRef]
14. Wu, S.-Q.; Yu, X.-K.; Lian, M.-L.; Park, S.-Y.; Piao, X.-C. Several factors affecting hypericin production of *Hypericum perforatum* during adventitious root culture in airlift bioreactors. *Acta Physiol. Plant.* **2014**, *36*, 975–981. [CrossRef]
15. Sobhani, A.; Khanahmadi, M.; Jalali, A.; Moradi, K.; Noormohammadi, N.; Ebrahimi, M. Development of a low-cost disposable bioreactor for pilot scale production of *Hypericum perforatum* L. adventitious roots. *Ind. Crops Prod.* **2020**, *160*, 113096. [CrossRef]
16. Gantait, S.; Mukherjee, E. Hairy root culture technology: Applications, constraints and prospect. *Appl. Microbiol. Biotechnol.* **2020**, *105*, 35–53. [CrossRef]
17. Vinterhalter, B.; Ninkovic, S.; Cingel, A.; Vinterhalter, D. Shoot and root culture of *Hypericum perforatum* L. transformed with Agrobacterium rhizogenes A4M70GUS. *Biol. Plant.* **2006**, *50*, 767–770. [CrossRef]
18. Komarovská, H.; Giovannini, A.; Košuth, J.; Čellárová, E. Agrobacterium rhizogenes-Mediated Transformation of *Hypericum tomentosum* L. and *Hypericum tetrapterum* Fries. *Z. Nat. C* **2009**, *64*, 864–868. [CrossRef]
19. Tusevski, O.; Stanoeva, J.; Stefova, M.; Kungulovski, D.; Pancevska, N.; Sekulovski, N.; Panov, S.; Simic, S. Hairy roots of *Hypericum perforatum* L.: A promising system for xanthone production. *Open Life Sci.* **2013**, *8*, 1010–1022. [CrossRef]
20. Zubrická, D.; Mišianiková, A.; Henzelyová, J.; Valletta, A.; De Angelis, G.; D'Auria, F.D.; Simonetti, G.; Pasqua, G.; Čellárová, E. Xanthones from roots, hairy roots and cell suspension cultures of selected Hypericum species and their antifungal activity against *Candida albicans*. *Plant Cell Rep.* **2015**, *34*, 1953–1962. [CrossRef]
21. Koperdáková, J.; Komarovská, H.; Košuth, J.; Giovannini, A.; Čellárová, E. Characterization of hairy root-phenotype in transgenic *Hypericum perforatum* L. clones. *Acta Physiol. Plant.* **2008**, *31*, 351–358. [CrossRef]
22. Komarovská, H.; Košuth, J.; Giovannini, A.; Smelcerovic, A.; Zuehlke, S.; Čellárová, E. Effect of the Number of rol Genes Integrations on Phenotypic Variation in Hairy Root-Derived *Hypericum perforatum* L. Plants. *Z. Nat. C* **2010**, *65*, 701–712. [CrossRef]
23. Vinterhalter, B.; Zdravković-Korać, S.; Mitić, N.; Bohanec, B.; Vinterhalter, D.; Savić, J. Effect of sucrose on shoot regeneration in Agrobacterium transformed *Hypericum perforatum* L. roots. *Acta Physiol. Plant.* **2015**, *37*, 1–12. [CrossRef]
24. Tusevski, O.; Vinterhalter, B.; Milošević, D.K.; Soković, M.; Ćirić, A.; Vinterhalter, D.; Korać, S.Z.; Stanoeva, J.P.; Stefova, M.; Simic, S.G. Production of phenolic compounds, antioxidant and antimicrobial activities in hairy root and shoot cultures of *Hypericum perforatum* L. *Plant Cell Tissue Organ Cult.* **2016**, *128*, 589–605. [CrossRef]

25. Tusevski, O.; Stanoeva, J.P.; Stefova, M.; Spasenoski, M.; Simic, S.G. State of antioxidant systems and phenolic compounds' production in *Hypericum perforatum* L. hairy roots. *Acta Physiol. Plant.* **2019**, *41*, 132. [CrossRef]
26. Tusevski, O.; Todorovska, M.; Stanoeva, J.P.; Stefova, M.; Simic, S.G. In Vitro and in Silico Insights on the Biological Activities, Phenolic Compounds Composition of *Hypericum perforatum* L. Hairy Root Cultures. *Phyton* **2022**, *92*, 921–941. [CrossRef]
27. Sharma, P.; Padh, H.; Shrivastava, N. Hairy root cultures: A suitable biological system for studying secondary metabolic pathways in plants. *Eng. Life Sci.* **2012**, *13*, 62–75. [CrossRef]
28. Tusevski, O.; Stanoeva, J.P.; Stefova, M.; Simic, S.G. Phenolic Profile of Dark-Grown and Photoperiod-Exposed *Hypericum perforatum* L. Hairy Root Cultures. *Sci. World J.* **2013**, *2013*, 1–9. [CrossRef]
29. Mukherjee, C.; Sircar, D.; Chatterjee, M.; Das, S.; Mitra, A. Combating photooxidative stress in green hairy roots of Daucus carota cultivated under light irradiation. *J. Plant Physiol.* **2014**, *171*, 179–187. [CrossRef]
30. Singleton, V.L.; Rossi, J.A. Colorimetry of total phenolics with phosphomolybdic-phosphotungstic acid reagents. *Am. J. Enol. Vitic.* **1965**, *16*, 144–158.
31. Zhishen, J.; Mengcheng, T.; Jianming, W. The determination of flavonoid contents in mulberry and their scavenging effects on superoxide radicals. *Food Chem.* **1999**, *64*, 555–559. [CrossRef]
32. Arnous, A.; Makris, D.P.; Kefalas, P. Correlation of Pigment and Flavanol Content with Antioxidant Properties in Selected Aged Regional Wines from Greece. *J. Food Compos. Anal.* **2002**, *15*, 655–665. [CrossRef]
33. Meyers, K.J.; Watkins, C.B.; Pritts, M.P.; Liu, R.H. Antioxidant and Antiproliferative Activities of Strawberries. *J. Agric. Food Chem.* **2003**, *51*, 6887–6892. [CrossRef] [PubMed]
34. Das, J.R.; Bhat, S.G.; Gowda, L.R. Purification and Characterization of a Polyphenol Oxidase from the Kew Cultivar of Indian Pineapple Fruit. *J. Agric. Food Chem.* **1997**, *45*, 2031–2035. [CrossRef]
35. Apak, R.; Güçlü, K.; Özyürek, M.; Karademir, S.E. Novel Total Antioxidant Capacity Index for Dietary Polyphenols and Vitamins C and E, Using Their Cupric Ion Reducing Capability in the Presence of Neocuproine: CUPRAC Method. *J. Agric. Food Chem.* **2004**, *52*, 7970–7981. [CrossRef] [PubMed]
36. Brand-Williams, W.; Cuvelier, M.E.; Berset, C. Use of a free radical method to evaluate antioxidant activity. *LWT Food Sci. Technol.* **1995**, *28*, 25–30. [CrossRef]
37. Decker, E.A.; Welch, B. Role of ferritin as a lipid oxidation catalyst in muscle food. *J. Agric. Food Chem.* **1990**, *38*, 674–677. [CrossRef]
38. Sun, T. Antioxidant activities of buckwheat extracts. *Food Chem.* **2005**, *90*, 743–749. [CrossRef]
39. Hemeda, H.M.; Klein, B.P. Effects of Naturally Occurring Antioxidants on Peroxidase Activity of Vegetable Extracts. *J. Food Sci.* **1990**, *55*, 184–185. [CrossRef]
40. Aebi, H. [13] Catalase in vitro. In *Methods in Enzymology*; Academic Press: Cambridge, MA, USA, 1984; Volume 105, pp. 121–126. [CrossRef]
41. Beauchamp, C.; Fridovich, I. Superoxide dismutase: Improved assays and an assay applicable to acrylamide gels. *Anal. Biochem.* **1971**, *44*, 276–287. [CrossRef]
42. Sergiev, I.; Alexieva, V.; Karanov, E. Effect of spermine, atrazine and combination between them on some endogenous protective systems and stress markers in plants. *Comptes Rendus Acad. Bulg. Sci.* **1997**, *51*, 121–124. [CrossRef]
43. Elstner, E.F.; Heupel, A. Inhibition of nitrite formation from hydroxylammoniumchloride: A simple assay for superoxide dismutase. *Anal. Biochem.* **1976**, *70*, 616–620. [CrossRef] [PubMed]
44. Heath, R.L.; Packer, L. Photoperoxidation in isolated chloroplasts: I. kinetics and stoichiometry of fatty acid peroxidation. *Arch. Biochem. Biophys.* **1968**, *125*, 189–198. [CrossRef] [PubMed]
45. Abdelkader, M.S.A.; Lockwood, G.B. Volatile oils from the plant and hairy root cultures of *Ageratum conyzoides* L. *Nat. Prod. Res.* **2011**, *25*, 909–917. [CrossRef]
46. Kino-oka, M.; Nagatome, H.; Taya, M. Characterization and application of plant hairy roots endowed with photosynthetic functions. In *Plant Cells*; Zhong, J.-J., Ed.; Springer: Berlin/Heidelberg, Germany, 2001; Volume 72, pp. 183–218. [CrossRef]
47. Taya, M.; Sato, H.; Kino-Oka, M.; Tone, S. Characterization of pak-bung green hairy roots cultivated under light irradiation. *J. Ferment. Bioeng.* **1994**, *78*, 42–48. [CrossRef]
48. Lanoue, A.; Boitel-Conti, M.; Dechaux, C.; Laberche, J.C.; Christen, P.; Sangwan-Norreel, B. Comparison of growth proper-ties, alkaloid production and water uptake of two selected Datura hairy root lines. *Acta Biol. Crac. Ser. Bot.* **2004**, *46*, 185–192.
49. Sidwa-Gorycka, M.; Krolicka, A.; Orlita, A.; Maliński, E.; Golebiowski, M.; Kumirska, J.; Chromik, A.; Biskup, E.; Stepnowski, P.; Lojkowska, E. Genetic transformation of *Ruta graveolens* L. by Agrobacterium rhizogenes: Hairy root cultures a promising approach for production of coumarins and furanocoumarins. *Plant Cell Tissue Organ Cult.* **2009**, *97*, 59–69. [CrossRef]
50. Abbasi, B.H.; Tian, C.-L.; Murch, S.J.; Saxena, P.K.; Liu, C.-Z. Light-enhanced caffeic acid derivatives biosynthesis in hairy root cultures of Echinacea purpurea. *Plant Cell Rep.* **2007**, *26*, 1367–1372. [CrossRef]
51. Dixon, R.A.; Achnine, L.; Kota, P.; Liu, C.-J.; Reddy, M.S.S.; Wang, L. The phenylpropanoid pathway and plant defence-a genomics perspective. *Mol. Plant Pathol.* **2002**, *3*, 371–390. [CrossRef]
52. Murthy, H.N.; Kim, Y.-S.; Park, S.-Y.; Paek, K.-Y. Hypericins: Biotechnological production from cell and organ cultures. *Appl. Microbiol. Biotechnol.* **2014**, *98*, 9187–9198. [CrossRef]
53. Qian, J.; Wu, J.; Yao, B.; Lu, Y. Preparation of a polyclonal antibody against hypericin synthase and localization of the enzyme in red-pigmented *Hypericum perforatum* L. plantlets. *Acta Biochim. Pol.* **2012**, *59*, 639–645. [CrossRef] [PubMed]

54. Pourcel, L.; Routaboul, J.-M.; Cheynier, V.; Lepiniec, L.; Debeaujon, I. Flavonoid oxidation in plants: From biochemical properties to physiological functions. *Trends Plant Sci.* **2007**, *12*, 29–36. [CrossRef] [PubMed]
55. Beaulieu, M.; D'Aprano, G.; Lacroix, M. Effect of dose rate of gamma irradiation on biochemical quality and browning of mushrooms Agaricus bisporus. *Radiat. Phys. Chem.* **2002**, *63*, 311–315. [CrossRef]
56. Gill, S.S.; Tuteja, N. Reactive oxygen species and antioxidant machinery in abiotic stress tolerance in crop plants. *Plant Physiol. Biochem.* **2010**, *48*, 909–930. [CrossRef]
57. Nagatome, H.; Tsutsumi, M.; Kino-Oka, M.; Taya, M. Development and characterization of a photoautotrophic cell line of pak-bung hairy roots. *J. Biosci. Bioeng.* **2000**, *89*, 151–156. [CrossRef] [PubMed]